Huang et al., Med chem 2015, 5:1
DOI: 10.4172/2161-0444.1000242

Medicinal chemistry

Research Article Open Access

Surface Modification of Superparamagnetic Magnetite Nanoparticles and Its Application for Detection of Anti-CEA Using Electrochemiluminescent Immunosensor

Guixin Huang, Biyang Deng*, Qing Xi, Chunyao Tao and Li Ye

Key Laboratory for the Chemistry and Molecular Engineering of Medicinal Resources (Ministry of Education of China), School of Chemistry and Pharmaceutical Sciences, Guangxi Normal University, Guilin 541004, China

Abstract

A highly sensitive sandwich-type ECLIA technique using ruthenium complexes as labels was reported. Superparamagnetic nanoparticles were synthesized with a diameter of 12 nm through a coprecipitation method and used as the matrix solid-phase. Then, the ECL targets of $Ru(bpy)_2(dcbpy)NHS$ were successfully synthesized and labeled on the IgG. Furthermore, on the formation of an antibody-antigen immunocomplex, biotin-streptavidin system and on the basis of the strong and stable ECL signal, we designed a novel multiple signal amplification of sandwich-type ECLIA for sensitive detection of carcinoembryonic antigen (CEA) antibody. The calibration curve was linear in the range of 1.0–780 ng mL^{-1} with a detection limit of 0.28 ng mL^{-1} (σ = 3) and relative standard deviation of 3.9% (n = 6). The results indicated that the new sandwich-type ECLIA provide several advantages, such as high sensitivity, good selectivity, and wide linear range. This technique can be used in detection of anti-CEA as well as of other tumor markers.

Keywords: Electrochemiluminescence; Sandwich-type immunoreactions; Magnetic nanoparticle; Tumor marker; Carcinogenesis

Introduction

Malignant tumor, a malignant disease, is a serious threat to human health and life. However, early diagnosis and effective therapy of malignant disease have been the main cause of decrease in mortality [1-3]. Tumor markers (TMs) as a vital important indicator, play an important role in early diagnosis of malignant disease. There have been more than one hundred of tumor markers; for example, the tumor-associated membrane protein [4-8], tumor-associated carbohydrate antigens [9-11], and enzymes and hormone [12,13]. Carcinoembryonic antigen (CEA), as a broad spectrum tumor marker, has been applied in the clinical examination to predict several cancer diseases, such as colon, lung, pancreatic, breast, and gastric cancers [14-16]. So far, some immunoassay methods have been used for clinical sample measurements [17-20]. In comparison with the other methods, such as radioimmunoassay [21], fluorescence immunoassay [22], chemiluminescence immunoassay [23], and enzyme-linked immunosorbent assay (ELISA) [24], the electrochemiluminescence immunoassay (ECLIA) method has considerable advantages, including lack of radioactive pollution, high sensitivity, good selectivity, wide linear range, good stability, fast inspection speed, high automation, and wide application range [25]. In recent years, with the development of nanoscience and nanotechnology, nanoparticles have been applied as the labels in different field [26-30]. Magnetic nanoparticles have revealed unique physical, chemical, thermal, and magnetic properties that made them attractive in many applications [31-34]. Electrochemiluminescence (ECL) is the production of light as the result of highly energetic electron transfer reactions between reactants in an electrochemical process. It has recently become available as an important technique in analytical chemistry [35,36]. The ECLIA is a new generation immunolabelling technique with the advantages of magnetic beads, immunoassay, and ECL [37,38]. On the basis of these outstanding advantages, ECLIA technique has been widely used in immunoassay, cell separation, DNA, and drug delivery systems [39-47].

In this work, we successfully assembled a highly sensitive analyzer of immunomagnetic electrochemiluminescence (IM-ECL). A novel analytical method for carcinoembryonic antibody detection was developed using electrochemiluminescence, immunoassay, biotin-avidin, and magnetic nanoparticle. The magnetic nanoparticles were synthesized using coprecipitation method, which were later coated onto (3-aminopropyl) triethoxysilane (APTES). Because of the outstanding integration of the strepavidin-biotin signal amplification with the high sensitivity of the ECL technique, a novel sandwich ECL immunoassay was constructed. The results indicated that the ECLIA technique exhibited no radioactive pollution, good selectivity, high sensitivity, wide linear range. It also provided excellent applicability in other tumor marker detections.

Materials and Methods

Materials and reagents

The primary anti-CEA monoclonal antibodies (Ab1) and the secondary anti-CEA (Ab2) were obtained from Biocell (Zhengzhou, China). Human serum albumin (HSA) and IgG were purchased from Beijing Dingguo Changsheng Biotechnology (Beijing, China). 4,4'-dicarboxylic acid-2,2'-bipyridine (dcbpy) and Tris(2,2′-bipyridyl)-ruthenium(II) chloride hexahydrate were obtained from Alfa Aesar (Ward Hill, MA, USA). (2,2'-bipyridyl) ruthenium dichloride and Tween-20 were purchased from J&K Chemical (Beijing, China). N,N'-dicyclohexyl carbodiimide (DCC), and N-hydroxysuccinimide (NHS) were obtained from Aladdin Reagent (Shanghai, China).

***Corresponding author:** Biyang Deng, Key Laboratory for the Chemistry and Molecular Engineering of Medicinal Resources (Ministry of Education of China), School of Chemistry and Pharmaceutical Sciences, Guangxi Normal University, Guilin 541004, China, Tel: +86-773-5845726; Fax: +86-773-2120958; E-mail: dengby16@163.com

Received December 17, 2014; **Accepted** January 29, 2015; **Published** January 31, 2015

Citation: Huang G, Deng B, Xi Q, Tao C, Ye L (2015) Surface Modification of Superparamagnetic Magnetite Nanoparticles and Its Application for Detection of Anti-CEA Using Electrochemiluminescent Immunosensor. Med chem 5: 050-057. doi:10.4172/2161-0444.1000242

Dimethyl Formamide (DMF), sodium hexafluorophosphate ($NaPF_6$), Tripropylamine (TPA), and Biotin-NHS were obtained from Sigma-Aldrich (St. Louis, MO, USA). Strepavidin was obtained from Sangon Biotech (Shanghai, China). Glutaraldehyde and ethanolamine were purchased from Sinopharm Chemical Reagent (Beijing, China). Sodium bicarbonate, sulfuric acid, and methanol were purchased from Guangzhou Chemical Reagent Factory (Guangzhou, China). The buffer used was a phosphate system (Na_2HPO_4/NaH_2PO_4, 0.05 mol L^{-1}, pH 7.4) obtained from Hunan Reagent Company (Hunan, China). All chemicals used in the experiments were of analytical grade and double-distilled water (DDW) was used throughout.

Characterizations and apparatus

The ECLIA examinations were carried out with MPI-B ECL system (Xi'an Remex Electronics Science & Technology, Xi'an, China) with a three-electrode system composed of a working electrode (platinum wire, 0.5 mm in diameter), a counter electrode (platinum wire), and an Ag/AgCl reference electrode. It was used in a conventional three-electrode system to produce $Ru(bpy)_3^{3+}$, which was reacted with the analytes to produce light. Transmission electron microscopy (TEM) images were obtained using a JEM-2100 microscope (JEOL, Japan). IR spectrometry examinations were performed on Fourier transform infrared spectrometry (FT–IR, Perkin Elmer, USA) system. Powder X-ray diffraction (XRD) patterns were acquired from dried nanoparticle samples with a Rigaku D/max 2500v/pc X-ray diffractometer (Rigaku, Japan). A MPMS-XL-7 vibrating sample magnetometer (VSM) (*Quantum Design,* USA) system was used to examine the magnetization of magnetite nanoparticles at room temperature. UV–vis spectra were measured on a Perkin-Elmer Lambda 35 UV–vis spectrometer (Perkin-Elmer, USA). For preparation of samples, a SK3200H ultrasonic cleaner (Shanghai Kudos Ultrasonics Instrument, Shanghai, China) was used.

Preparation of Fe_3O_4 magnetic nanoparticles (MNPs)

Iron oxide (Fe_3O_4) nanoparticles were synthesized via a coprecipitation method. A aqueous solution consisting of ferric chloride (0.0875 mol L^{-1}) and ferrous chloride tetrahydrate (0.05 mol L^{-1}) was prepared under N_2 atmosphere. Then, aqueous solution of ammonia (1.5 mol L^{-1}) was quickly dropped into the solution with mechanical stirring until the pH of the solution reached to 9~10. The reaction was performed at 80 °C, for 2 h. The obtained black precipitates were isolated via magnetic separation and washed with DDW and ethanol for several times until a pH of 7 was reached. The chemical reaction of Fe_3O_4 precipitation may be considered as follows:

$$Fe^{2+} + 2Fe^{3+} + 8OH^- \rightarrow Fe_3O_4 + 4H_2O$$

Surface modification of MNP with APTES

100 mg Magnetite nanoparticles coated with 250 mg APTES ($(NH_2(CH_2)_3Si(OC_2H_5)_3$) via a silanization reaction to obtain a large number of amino groups on the surface of MNPs [48,49]. In the process, the magnetite is suspensed in 150 mL ethanol:water (1:1, v:v) solution with sonication for 30 min to obtain a uniform dispersion. Then, a certain amount of APTES was added to the solution with mechanical stirring. The solution was protected under N_2 at 60 °C for 2 h. The molar ratio of APTES to Fe_3O_4 was 4:1. After the reaction completed, the solution was cooled to room temperature and isolated through magnetic separation method. In the sequence, the finalized magnetite particles were thoroughly washed with ethanol, followed by DDW and dried under vacuum at 70°C for 24 h.

Synthesis of $Ru(bpy)_2(dcbpy)NHS$

The synthetic pathway of the activated NHS ester of $Ru(bpy)_2(dcbpy)NHS$ is shown in Figure 1a and b. It was prepared in two steps according to the literatures [50,51] with some modifications. Briefly, $Ru(bpy)_2Cl_2$ (0.2 g), 2,2'-bipyridine4,4'-dicarboxylic acid (dcbpy) (0.12 g), and $NaHCO_3$ (0.2 g) were dissolved in 40 mL of 80% methanol:water (*v:v*) solution and mixed under reflux at 80°C for 10 h. Then, the solution was cooled in an ice bath for 2 h. Sulfuric acid (1 M) was slowly dropped into the mixing solution to adjust pH to 4.4. The formed precipitate was filtrated through vacuum filtration and washed three times with 10 mL of methanol. Finally, 10 mL of $NaPF_6$ solution was added into the filter liquor with magnetic stirring for 30 min. The solution was cooled to 4°C inside refrigerator for 10 days. The formed

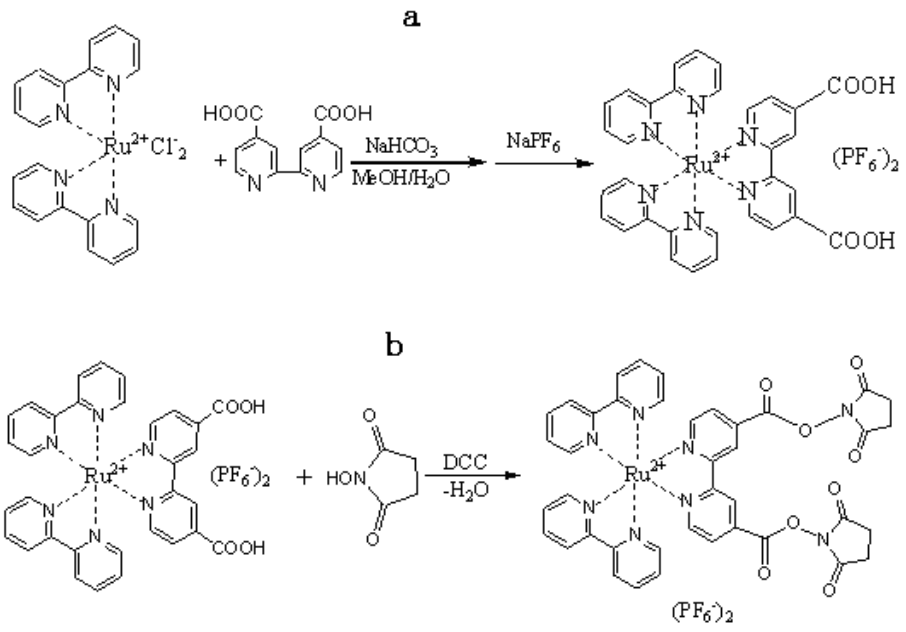

Figure 1: Synthetic routes of: (a) Ru(bpy)2(dcbpy)(PF6)2; (b) Ru(bpy)2(dcbpy)NHS.

crystals were collected via vacuum filtration and recrystallized from methanol. The obtained crystal was $Ru(bpy)_2(dcbpy)(PF6)_2$.

After the first step that the reaction completed, DCC (0.46 g) and NHS (0.24 g) were dissolved in 4.0 mL of DMF with magnetic stirring and cooled in an ice bath. Next, the solution of $Ru(bpy)_2(dcbpy)(PF_6)_2$ (0.146 g) in 1 mL of DMF was added and the mixture was stirred for 5 h. The formed precipitate was removed through vacuum filtration and the filtrate, containing $Ru(bpy)_2(dcbpy)NHS$, was used for the ECL labeling. Finally, the ECL targets of $Ru(bpy)_2(dcbpy)NHS$ was estimated at 2.65×10^{-2} mol L^{-1} with UV–vis absorption measurement.

Streptavidin immobilization on MNPs

Streptavidin immobilization on the magnetite nanoparticles was conducted according to the method reported in literatures with some modification [52-54]. Typically, Fe_3O_4/APTES (50 mg) was dispersed via sonication into a 10 mL 10% glutaraldehyde solution in 0.05 mol L^{-1} phosphate buffer solution (PBS, pH 7.4), and then stirred repercussion for 3 h at room temperature. The suspension was washed three times in this manner with PBS (pH 7.4) through magnetic separation method. A solution of 10 mg Fe_3O_4/APTES mixed with 1 mL of 0.05 mol L^{-1} PBS (pH 7.4) containing 0.5% Tween-20 was transferred into a 5.0 mL centrifuge tube. One milliliter of 0.05 mol L^{-1} PBS (pH 7.4) containing 1.0 mg Streptavidin (SA) was added to the above mixing solution, which was incubated for 10 h at 4°C while stirring. After that, the solution was allowed to add excess ethanolamine (0.2 mL, 1.0 mol L^{-1}) and stirred for 2 h at room temperature. This procedure was performed to terminate the activated residual groups. After the reaction was completed, the bead conjugates were washed five times with PBS. Finally, the bead conjugates were re-suspended in 1.0 mL of 0.05 mol L^{-1} PBS (pH 7.4) containing 0.5% Tween 20 (pH 7.4). Unreacted streptavidin was analyzed with the UV absorption at 282 nm.

Preparation of biotinylated anti-CEA

A 1.0 mg of Biotin-N-hydroxysuccinimide ester (BNHSE) was dissolved in dimethyl sulfoxide. Anti-CEA monoclonal antibodies (1.0 mg) was added to 100 mmol L^{-1} sodium bicarbonate solution (pH 8.3) and then reacted with 75 μg of BNHSE. The reaction mixture was incubated for 4 h at room temperature on an end-over-end rotator. They were then transferred to centrifugal tube using centrifugal ultrafiltration to remove unreacted materials. Finally, sodium bicarbonate solution was added to the conjugate to a total reaction volume of 1.0 mL.

Preparation of $Ru(bpy)_2(dcbpy)NHS$ labeled IgG

The $Ru(bpy)_2(dcbpy)NHS$ labeled IgG was made via mixing 2.0 mg of IgG in 2.0 mL of PBS (pH 7.8) with freshly prepared 120 μL of 2.65×10^{-2} mol L^{-1} $Ru(bpy)_2(dcbpy)NHS$ in DMF, while incubated under shaking in a 37°C water bath for 6 h in the dark. Then, the mixing solution was transferred into the centrifuge tube via centrifugal ultrafiltration-dialysis. The purified $Ru(bpy)_2(dcbpy)NHS$ labeled IgG was further diluted with PBS (pH 7.8) to 2.0 mL and stored at 4°C in the dark.

Fabrication of sandwich-type ECL immunocomplexes

Figure 2 schematically shows the designed ECLIA technique for anti-CEA. The immunocomplexes were prepared as follows: A mixture of 1.0 mL biotinylated anti-CEA (Ab1) and 1.0 mL streptavidin-coated magnetic beads was prepared and incubated at room temperature for 1 h. After that, the mixed solution was washed twice with PBST (0.01 M pH 7.8 PBS containing 0.05% Tween-20) via magnetic separation, then was dispersed in 0.01 M of PBS to a final volume of 2.0 mL. Subsequently, 1.0 mg of human serum albumin (HSA) was added and incubated at room temperature for 30 min under stirring. After washing with PBS, the components were dissolved in 0.01 M of PBS to a final volume of 3.0 mL. Finally, the mixing solution was incubated with anti-CEA (Ab2) and Ru(bpy)2(dcbpy)NHS labeled IgG. After the reaction completed, it was washed with PBST via magnetic separation and was used for the ECL examination.

ECL measurements

The ECL detection for anti-CEA was performed via IM-ECL measurements, as shown in Figure 3. The heart of the ECL system is the reaction cell and light signal acquisition device. The reaction cell, which produces ECL signal, contains a working electrode, a counter electrode, and an Ag/AgCl reference electrode. The process of IM-ECL measurement is shown in Figure 4. The magnetic sandwich-type immunocomplex solutions, with various concentrations of target anti-CEA and a solution of PBST containing 0.01 M TPA, were added to the reaction cell, where the magnetic beads were captured on the surface of the working electrode by a magnet above it. Then, a voltage of 1.25 V was applied to the working electrode and counter electrode, and a voltage of 800 V to the photomultiplier tube. In this way, the ECL signals related to the anti-CEA concentrations could be measured.

Results and Discussion

Identification of MNP

In the present study, Fe_3O_4 magnetic nanoparticles were synthesized via chemical coprecipitation process. The surface of Fe_3O_4 MNPs were chemically modified with APTES. The morphology and properties of these magnetic nanoparticles were characterized with

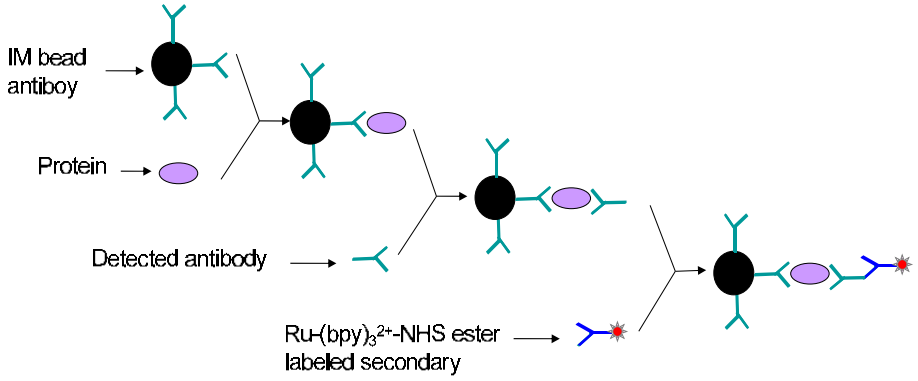

Figure 2: Process schematic of immunoassay. IM for immunomagnetic, NHS for N-hydroxysuccinimide.

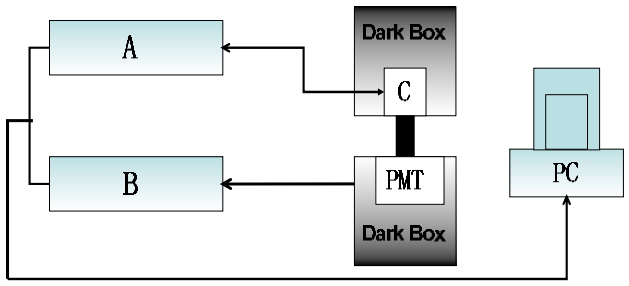

Figure 3: Design diagram of immunomagnetic electrochemiluminescence analyzer. A: Electrochemical controlling system; B: Multi-function chemiluminescence collector; C: Electrochemiluminescence reaction cell; PMT: Photomultiplier tube; PC: Personal computer. The C and PMT were placed in dark boxes, respectively.

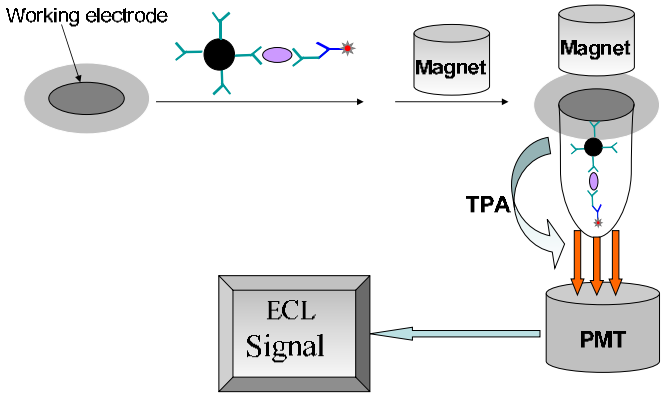

Figure 4: Process of IM-ECL measurements. TPA for tripropylamine, PMT for Photomultiplier tube, ECL for Electrochemiluminescence.

TEM, XRD, FT–IR spectrometry, and VSM techniques. The FT–IR spectra in Figure 5a show that the APTES was successfully coated on the Fe_3O_4 MNPs surfaces. The size distribution and average diameter of the MNPs were manipulated to about 12.5 nm based on the observations of TEM (Figure 5b). Most particles in the micrograph appear spherical although some aggregations of particles are seen. In this work, the magnetic properties of the MNPs were analyzed using VSM technique. Figure 5c shows a typical magnetization curve of MNPs, revealing hysteresis loop of MNP at room temperature. The curve exhibits zero remanence and coercivity, indicating that MNPs possess superparamagnetic properties and includes single-domain nanoparticles. The saturation magnetization of the magnetite was determined as 71 emu g^{-1}. The large saturation magnetization value of MNP makes it very susceptible to magnetic fields, and therefore, makes it easily separated from the solid and liquid phase. The synthesized MNPs provided good superparamagnetism. The XRD patterns of synthesized MNPs are shown in Figure 5d, confirming the existence of crystalline structure in the MNPs. The XRD pattern of MNPs exactly matched to the reference pattern of magnetite Fe_3O_4 provided by the Joint Committee on Powder Diffraction Standards (JCPDS) database PDF No. 65-3107. On the basis of the above results, the synthesized Fe_3O_4 MNPs could be used in the following experiment.

Characteristics of $Ru(bpy)_2(dcbpy)NHS$ and $Ru(bpy)_2(dcbpy)$ NHS labeled IgG

Properties of synthesized ruthenium complex: The structural formula of ruthenium complex of Ru-bis(2,2'-bipyridine) (dicarboxylic acid-2,2'-bipyridine-4,4') N-hydroxysuecinimide ester ($Ru(bpy)_2(dcbpy)NHS$) is shown in Figure 6, which was synthesized according to the method described in the experimental section. The $Ru(bpy)_2$ (dcbpy)NHS was characterized with FT–IR, UV–vis, and fluorescent spectrometry techniques. The FT–IR spectra of Ru-$(bpy)_2(dcbpy)NHS$ is shown in Figure 7. In these spectra, the 846

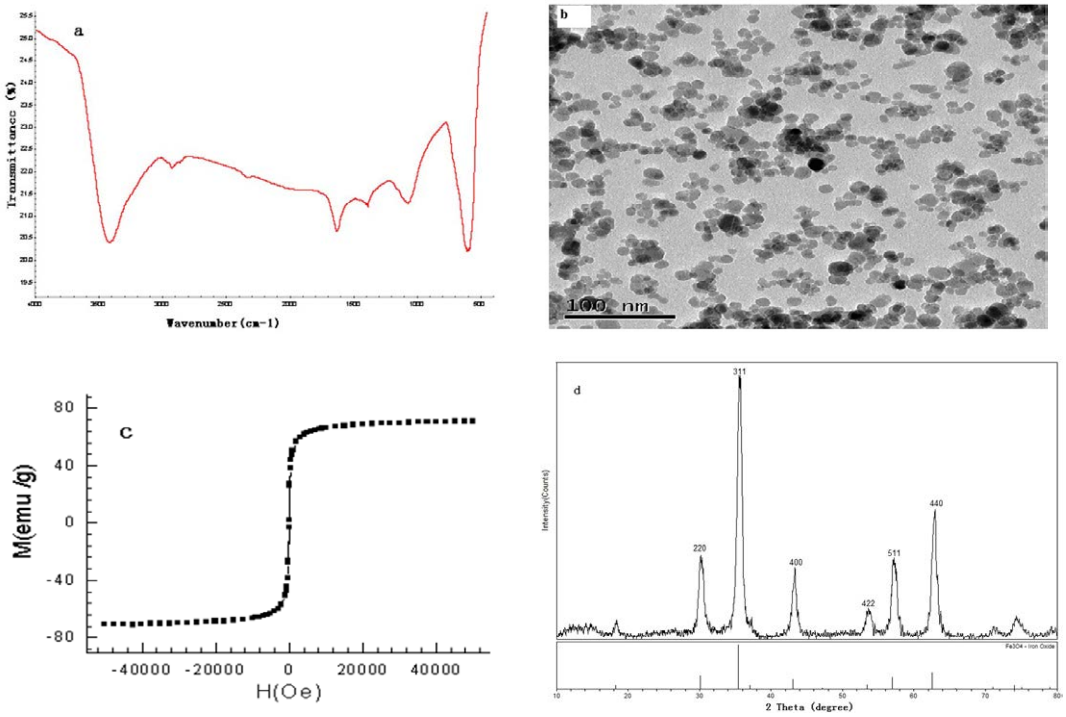

Figure 5: (a) FT–IR spectra of Fe_3O_4/APTES magnetic nanoparticles; (b) TEM micrograph of Fe_3O_4/APTES magnetic nanoparticles; (c) Magnetization curves of Fe_3O_4/APTES magnetic nanoparticles; (d) XRD pattern of Fe_3O_4/APTES magnetic nanoparticles.

cm^{-1} band belongs to the stretching vibration mode of =C–H bonds. Absorption bands at 1224 cm^{-1} for stretching vibration of –C–O bond, bands at 1712 and 1778 cm^{-1}, corresponding to –C=O groups, were observed.

The fluorescence spectra properties of $Ru(bpy)_2(dcbpy)NHS$ are presented in Figure 8a and b. $Ru(bpy)_2(dcbpy)NHS$ exhibits the characteristic of metal-to-ligand charge-transfer band centered at 456 nm in the excitation spectrum. The same characteristic was found in $Ru(bpy)_3^{2+}$. The π–π* transition of bipyridine is present at 280 nm. $Ru(bpy)_2(dcbpy)NHS$ revealed a maximum excitation wavelength at 465 nm and a maximum emission wavelength at 625 nm. The investigation was carried out in PBS. Furthermore, the ECL behavior of $Ru(bpy)_2(dcbpy)NHS$ was detected. The cyclic voltammograms and the corresponding ECL intensities of the $Ru(bpy)_2(dcbpy)NHS$ and $Ru(bpy)_3^{2+}$ are shown in Figure 9a-d. Good luminescent properties with $Ru(bpy)_2(dcbpy)NHS$ was observed. Simultaneously, the ECL performance of $Ru(bpy)_2(dcbpy)NHS$ was found stable. All of these observations revealed that the synthesis of $Ru(bpy)_2(dcbpy)NHS$ was successful.

ECL behavior of $Ru(bpy)_2(dcbpy)NHS$ labeled IgG: Cyclic voltammetry technique and the corresponding ECL emission were used to characterize the electrochemical and ECL behaviors of IgG,

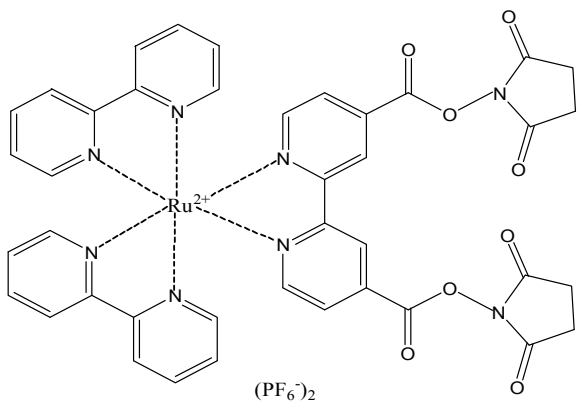

Figure 6: Structural formula of $Ru(bpy)_2(dcbpy)NHS$.

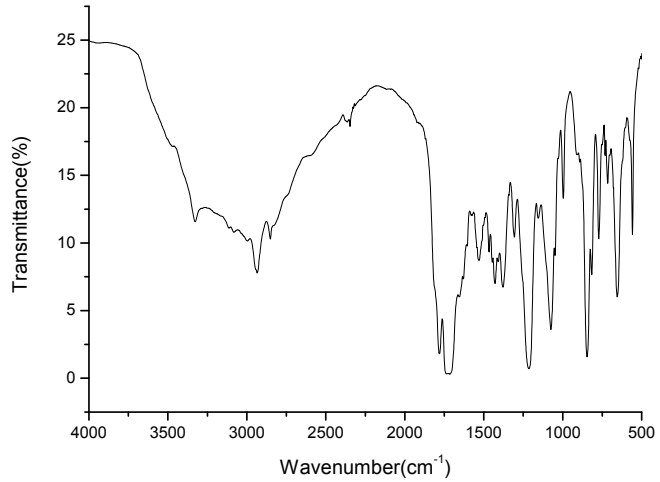

Figure 7: FT–IR spectra of drying of $Ru(bpy)_2(dcbpy)NHS$. (a) 846.22 cm^{-1} band for the stretching vibration mode of =C–H bonds; (b) bands in 1223.61 cm^{-1} due to stretching vibration of –C–O bond; (c,d) the bands in 1710.64 cm^{-1} and 1777.78 cm^{-1} corresponding to –C=O groups.

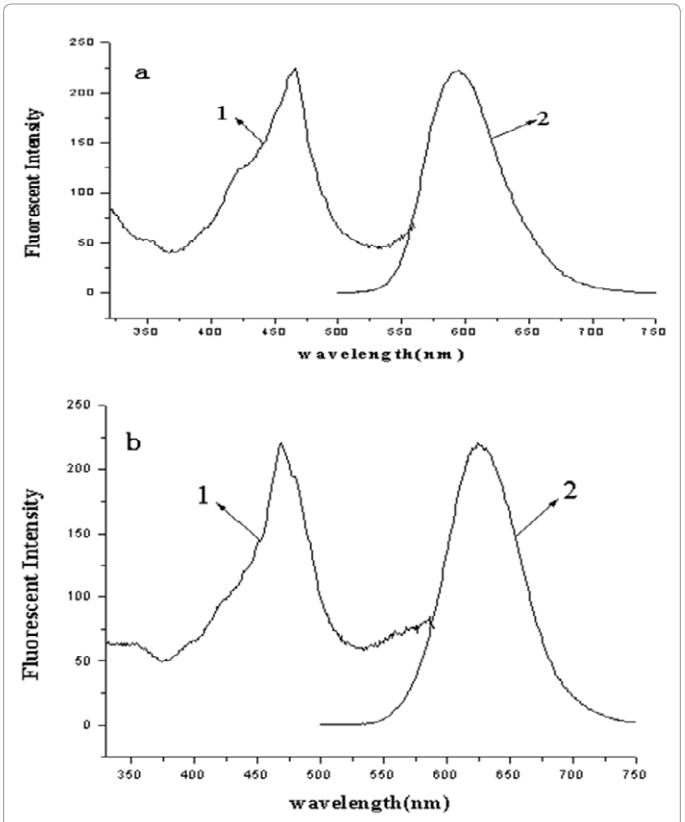

Figure 8: (a) Fluorescence spectra of $Ru(bpy)_3C1_2$; (b) $Ru(bpy)_2(dcbpy)NHS$. 1: Excitation spectrum; 2: Emission spectrum. (Detection conditions: Slit width 5 nm, excitation wavelength: 465 nm).

$Ru(bpy)_3^{2+}$, and $Ru(bpy)_2(dcbpy)NHS$ labeled IgG. The ECL behaviors of these materials were studied from starting at approximately 0.20 to the ending at 1.5 V. There was an obvious rise at about 1.25 V in the presence of TPA for $Ru(bpy)_3^{2+}$ and $Ru(bpy)_2(dcbpy)NHS$ labeled IgG. Simultaneously, there was no rise at about 1.25 V for IgG (Figure 10). The results showed that $Ru(bpy)_2(dcbpy)NHS$ was successfully labeled on the IgG and kept the ECL properties of $Ru(bpy)_3^{2+}$.

Performance of the Immunomagnetic sandwich-type ECL for anti-CEA detection

For each examination, sandwich-type immunocomplexes with various concentrations of anti-CEA and 100 μL ECL buffer solution containing 0.01 M TPA was added to the reaction cell and measurements were conducted with IM-ECL. Results indicated that the intensity of ECL increase with the concentrations of anti-CEA. The calibration curve (Figure 11) was linear over the range of 1.0–780 ng mL^{-1} with a detection limit of 0.28 ng mL^{-1} ($\sigma = 3$). The relative standard deviation was 3.9% (n = 6). The linearity range for the developed method is larger than that of the previous report [17,19]. The limit of detection of this method is higher than that of literature [18,20] and lower than that of reference [19].

Application to real samples

The feasibility of the developed sandwich type immunoassay for the detecting of CEA antibody was further evaluated using nine serum samples obtained from Guilin Medical University. The results showed that the concentrations of CEA antibody in these serum samples were between 0.9622 and 159.2 ng mL^{-1} (Table 1). CEA concentrations were measured by our developed immunoassay and compared with those

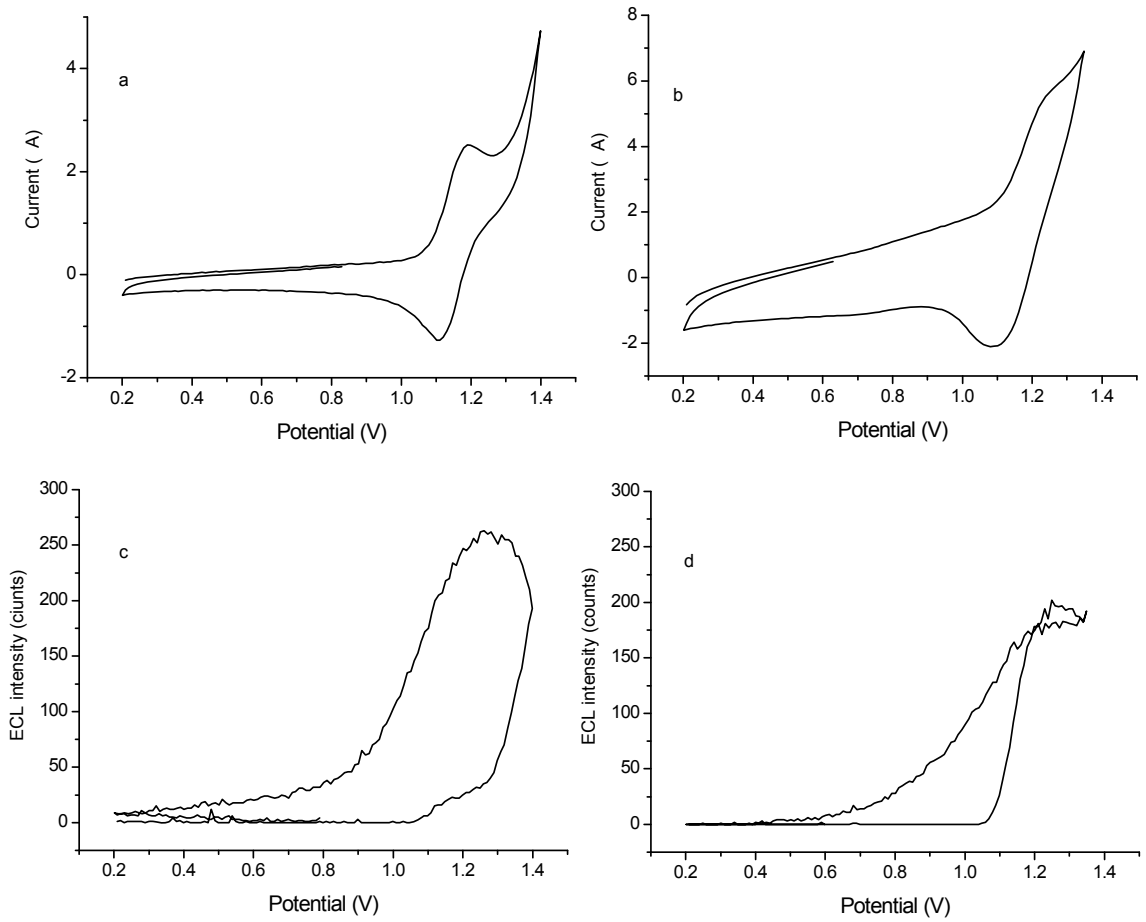

Figure 9: (a,b) Cyclic voltammograms; (c,d) profiles of electrogenerated chemiluminescence. Detection conditions: (a) 5 mmol L^{-1} $Ru(bpy)_3C1_2$ + 50 mmol L^{-1} PBS (pH7.4), scan rate: 100 mV s^{-1}; (b) 5 mmol L^{-1} $Ru(bpy)_2$(dcbpy)NHS + 50 mmol L^{-1} PBS (pH7.4), scan rate: 100 mV s^{-1}; (c) 5 mmol L^{-1} $Ru(bpy)_3C1_2$ + 50 mmol L^{-1} PBS (pH7.4), scan rate: 100 mV s^{-1}; (d) 5 mmol L^{-1} $Ru(bpy)_2$(dcbpy)NHS + 50 mmol L^{-1} PBS (pH7.4), scan rate: 100 mV s^{-1}.

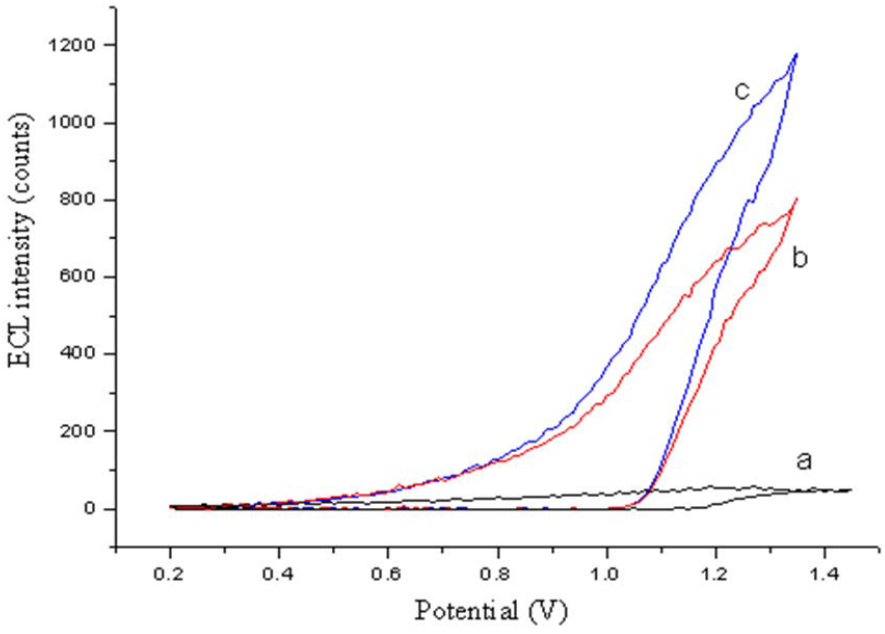

Figure 10: Profiles of electrochemiluminescence (ECL). (a) IgG; (b) $Ru(bpy)_2$(dcbpy)NHS labeled IgG; (c) 10 mmol L^{-1} $Ru(bpy)_3^{2+}$. Scan voltage: 0.2～1.5 V; scan rate: 100 mV s^{-1}.

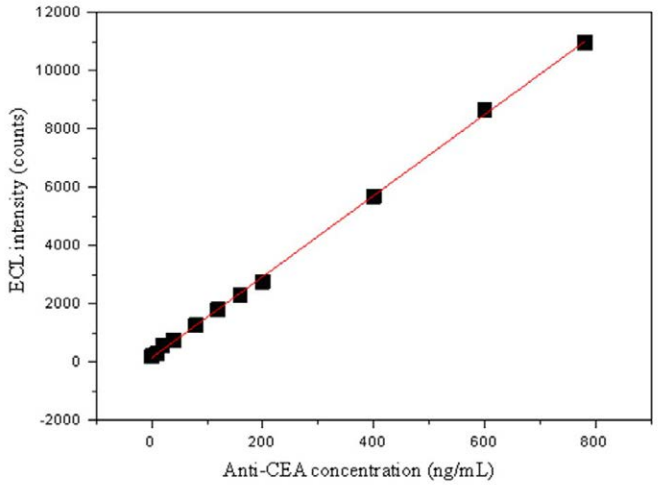

Figure 11: Relationships between of ECL signal and CEA antibody concentrations.

Samples	Found (ng/mL)	Added (ng/mL)	Total (ng/mL)	Recovery (%)
Serum 1	0.9622	1.000	1.86	95.78
Serum 2	1.214	1.200	2.35	96.33
Serum 3	14.93	15.00	29.4	96.47
Serum 4	30.25	30.00	60.8	101.8
Serum 5	43.81	45.00	89.6	101.8
Serum 6	62.72	60.00	121.7	98.3
Serum 7	123.4	120.0	242.1	98.92
Serum 8	134.6	130.0	263.5	99.15
Serum 9	159.2	160.0	320.6	100.9

Table 1: Analytical results of anti-CEA in human serum samples.(n = 6).

detected by a commercially available chemiluminescence method of Roche diagnosis. Linear regression analyses revealed good correlations between the developed method and chemiluminescence method of Roche diagnosis. The correlation coefficient was r=0.9951 between our proposed method and the commercially available chemiluminescence method of Roche diagnosis. This result indicated that no significant difference was found between the results of the two methods (paired t-test, P=0.214) and the proposed assay could serve for clinical determination of CEA in human serum.

Conclusions

In this paper, we assembled a highly sensitive analyzer of IM-ECL. On the basis of the new analyzer, we designed a novel analytical method for CEA antibody and developed using ECLIA, biotin-avidin, and MNP together. The method showed high sensitivity and reproducibility for the determination of CEA antibody in serum samples, suggesting its potential application value. This system could be also used for detection of other tumor markers.

Acknowledgments

This work was financially supported by the National Natural Science Foundation of China (Grant no. 21365006) and by the Guangxi Science Foundation of China (Grant no. 2014GXNSFDA118004).

References

1. Rusling JF, Kumar CV, Gutkind JS, Patel V (2010) Measurement of biomarker proteins for point-of-care early detection and monitoring of cancer. Analyst 135: 2496-2511.
2. Arya SK, Bhansali S (2011) Lung cancer and its early detection using biomarker-based biosensors. Chem Rev 111: 6783-6809.
3. Végvári A, Marko-Varga G (2010) Clinical protein science and bioanalytical mass spectrometry with an emphasis on lung cancer. Chem Rev 110: 3278-3298.
4. Wang L, Wei W, Han J, Fu Z (2012) Individually addressable electrode array for multianalyte electrochemiluminescent immunoassay based on a sequential triggering strategy. Analyst 137: 735-740.
5. Li C, Fu Z, Li Z, Wang Z, Wei W (2011) Cross-talk-free multiplexed immunoassay using a disposable electrochemiluminescent immunosensor array coupled with a non-array detector. Biosens Bioelectron 27: 141-147.
6. Sánchez-Carbayo M, Espasa A, Chinchilla V, Herrero E, Megías J, et al. (1999) New Electrochemiluminescent Immunoassay for the Determination of CYFRA 21-1: Analytical Evaluation and Clinical Diagnostic Performance in Urine Samples of Patients with Bladder Cancer. Clin Chem 45: 1944-1953.
7. Thompson I, McGiven J, Sawyer J, Thirlwall R, Commander N, et al. (2009) Competitive electrochemiluminescence wash and no-wash immunoassays for detection of serum antibodies to smooth Brucella strains. Clin Vaccine Immunol 16: 765-771.
8. Yan G, Xing D, Tan S, Chen Q (2004) Rapid and sensitive immunomagnetic-electrochemiluminescent detection of p53 antibodies in human serum. J Immunol Methods 288: 47-54.
9. Yuan S, Yuan R, Chai Y, Mao L, Yang X, et al. (2010) Sandwich-type electrochemiluminescence immunosensor based on Ru-silica@Au composite nanoparticles labeled anti-AFP. Talanta 82: 1468-1471.
10. Miao W, Bard AJ (2004) Electrogenerated chemiluminescence. 80. C-reactive protein determination at high amplification with [Ru(bpy)3]2+-containing microspheres. Anal Chem 76: 7109-7113.
11. Sardesai NP, Barron JC, Rusling JF (2011) Carbon nanotube microwell array for sensitive electrochemiluminescent detection of cancer biomarker proteins. Anal Chem 83: 6698-6703.
12. Zhou X, Xing D, Zhu D, Jia L (2009) Magnetic bead and nanoparticle based electrochemiluminescence amplification assay for direct and sensitive measuring of telomerase activity. Anal Chem 81: 255-261.
13. Fang L, Lü Z, Wei H, Wang E (2008) A electrochemiluminescence aptasensor for detection of thrombin incorporating the capture aptamer labeled with gold nanoparticles immobilized onto the thio-silanized ITO electrode. Anal Chim Acta 628: 80-86.
14. Ma JW, Fan Q, Wang L, Jia N, Gu Z, et al. (2010) Synthesis of magnetic and fluorescent bifunctional nanocomposites and their applications in detection of lung cancer cells in humans. Talanta 81: 1162-1169.
15. Song Z, Yuan R, Chai Y, Jiang W, Su H, et al. (2011) Simultaneous immobilization of glucose oxidase on the surface and cavity of hollow gold nanospheres as labels for highly sensitive electrochemical immunoassay of tumor marker. Biosens Bioelectron 26: 2776-2780.
16. Li H, Cao Z, Zhang Y, Lauand CW, Lu JZ (2010) Combination of quantum dot fluorescence with enzyme chemiluminescence for multiplexed detection of lung cancer biomarkers. Anal. Methods 2: 1236-1242.
17. Yu Q, Wang X, Duan Y (2014) Capillary-based three-dimensional immunosensor assembly for high-performance detection of carcinoembryonic antigen using laser-induced fluorescence spectrometry. Anal Chem 86: 1518-1524.
18. Miao X, Zou S, Zhang H, Ling L (2014) Highly sensitive carcinoembryonic antigen detection using Ag@Au core–shell nanoparticles and dynamic light scattering. Sensors and Actuator B19: 396-400.
19. Feng D, Li L, Fang X, Han X, Zhang Y (2014) Dual signal amplification of horseradish peroxidase functionalized nanocomposite as trace label for the electrochemical detection of carcinoembryonic antigen. Electrochim Acta 127: 334.
20. Li M, Zhang Y, Zhang M, Yan M, Ge S, et al. (2014) Monatshefte Für Chemie 145: 113.
21. Moon SH, Lee HY, Shin SY, Min GS, Lee HJ, et al. (2009) Nucl Med Mol Imaging 43: 323.
22. Yan F, Zhou J, Lin J, Ju H, Hu X (2005) Flow injection immunoassay for carcinoembryonic antigen combined with time-resolved fluorometric detection. J Immunol Methods 305: 120-127.
23. Li Z, Zhang Q, Zhao L, Li Z, Hu G, et al. (2009) Micro-platemagnetic chemiluminescence immunoassay and its applications incarcinoembryonic antigen analysis. Sci China Chem 53: 812-819.

24. Fu X (2008) Magnetic-controlled non-competitive enzyme-linked voltammetric immunoassay for carcinoembryonic antigen. Biochem Eng J 39: 267-275.

25. Miao W (2008) Electrogenerated chemiluminescence and its biorelated applications. Chem Rev 108: 2506-2553.

26. Maltas E, Ozmen M, Vural HC, Yildiz S, Ersoz M (2011) Immobilization of albumin on magnetite nanoparticles. Mater Lett 65: 3499-3501.

27. Maltas E, Ozmen M, Vural HC (2013) Mater Lett 106: 8.

28. Can K, Ozmen M, Ersoz M (2009) Immobilization of albumin on aminosilane modified superparamagnetic magnetite nanoparticles and its characterization. Colloids Surf B Biointerfaces 71: 154-159.

29. Buzoglu L, Maltas E, Ozmen M, Yildiz S (2014) Interaction of donepezil with human serum albumin on amine-modified magnetic nanoparticles. Coll & Surf A: Physicochem Engi Aspects 442: 139-145.

30. Maltas E, Ozmen M, Yildirimer B, Kucukkolbasi S, Yildiz S (2013) Interaction between ketoconazole and human serum albumin on epoxy modified magnetic nanoparticles for drug delivery. J Nanosci Nanotechnol 13: 6522-6528.

31. Trekker J, Leten C2, Struys T3, Lazenka VV4, Argibay B5, et al. (2014) Sensitive in vivo cell detection using size-optimized superparamagnetic nanoparticles. Biomaterials 35: 1627-1635.

32. Zong S, Wang Z, Chen H, Hu G, Liu M, et al. (2014) Colorimetry and SERS dual-mode detection of telomerase activity: combining rapid screening with high sensitivity. Nanoscale 6: 1808-1816.

33. Ren J, Tang D, Su B, Tang J, Chen G (2010) Glucose oxidase-doped magnetic silica nanostrutures as labels for localized signal amplification of electrochemical immunosensors. Nanoscale 2: 1244-1249.

34. Tudisco C, Bertani F, Cambria MT, Sinatra F, Fantechi E, et al. (2013) Functionalization of PEGylated Fe3O4 magnetic nanoparticles with tetraphosphonate cavitand for biomedical application. Nanoscale 5: 11438-11446.

35. Deng B, Lu H, Li L, Shi A, Kang Y, et al. (2010) Determination of the number of binding sites and binding constant between diltiazem hydrochloride and human serum albumin by ultrasonic microdialysis coupled with online capillary electrophoresis electrochemiluminescence. J Chromatogr A 1217: 4753-4756.

36. Deng B, Xu Q, Lu H, Ye L, Wang Y (2012) Pharmacokinetics and residues of tetracycline in crucian carp muscle using capillary electrophoresis on-line coupled with electrochemiluminescence detection. Food Chem 134: 2350-2354.

37. Zhang M, Ge S, Li W, Yan M, Song X, et al. (2012) Ultrasensitive electrochemiluminescence immunoassay for tumor marker detection using functionalized Ru-silica@nanoporous gold composite as labels. Analyst 137: 680-685.

38. Meng L, Gan N, Li T, Cao Y, Hu F, et al. (2011) A three-dimensional, magnetic and electroactive nanoprobe for amperometric determination of tumor biomarkers. Int J Mol Sci 12: 362-375.

39. Deiss F, LaFratta CN, Symer M, Blicharz TM, Sojic N, et al. (2009) Multiplexed sandwich immunoassays using electrochemiluminescence imaging resolved at the single bead level. J Am Chem Soc 131: 6088-6089.

40. Massart C, Sapin R, Gibassier J, Agin A, d'Herbomez M (2009) Intermethod Variability in TSH-Receptor Antibody Measurement: Implication for the Diagnosis of Graves Disease and for the Follow-Up of Graves Ophthalmopathy. Clin Chem 55: 183-186.

41. Jie G, Li L, Chen C, Xuan J, Zhu JJ (2009) Enhanced electrochemiluminescence of CdSe quantum dots composited with CNTs and PDDA for sensitive immunoassay. Biosens Bioelectron 24: 3352-3358.

42. Tian D, Duan C, Wang W, Cui H (2010) Ultrasensitive electrochemiluminescence immunosensor based on luminol functionalized gold nanoparticle labeling. Biosens Bioelectron 25: 2290-2295.

43. Hu S, Liu R, Zhang S, Huang Z, Xing Z, et al. (2009) A new strategy for highly sensitive immunoassay based on single-particle mode detection by inductively coupled plasma mass spectrometry. J Am Soc Mass Spectrom 20: 1096-1103.

44. Lin D, Wu J, Yan F, Deng S, Ju H (2011) Ultrasensitive immunoassay of protein biomarker based on electrochemiluminescent quenching of quantum dots by hemin bio-bar-coded nanoparticle tags. Anal Chem 83: 5214-5221.

45. He Y, Zhang H, Chai Y, Cui H (2011) DNA sensor by using electrochemiluminescence of acridinium ester initiated by tripropylamine. Anal Bioanal Chem 399: 3451-3458.

46. Wang X, Yun W, Dong P, Zhou J, He P, et al. (2008) A controllable solid-state Ru(bpy)(3)(2+) electrochemiluminescence film based on conformation change of ferrocene-labeled DNA molecular beacon. Langmuir 24: 2200-2205.

47. Carrozza C, Corsello SM, Paragliola RM, Ingraudo F, Palumbo S, et al. (2010) Clinical accuracy of midnight salivary cortisol measured by automated electrochemiluminescence immunoassay method in Cushing's syndrome. Ann Clin Biochem 47: 228-232.

48. Herrera AP, Barrera C, Rinaldi C (2008) Synthesis and functionalization of magnetite nanoparticles with aminopropylsilane and carboxymethyldextran. J Mater Chem 18: 3650-3654.

49. Van de Waterbeemd M, Sen T, Biagini S, Bruce IJ (2010) Surface functionalisation of magnetic nanoparticles: quantification of surface to bulk amine density. Micro Nano Lett 5: 282-285.

50. Terpetschnig E, Szmacinski H, Malak H, Lakowicz JR (1995) Metal-ligand complexes as a new class of long-lived fluorophores for protein hydrodynamics. Biophys J 68: 342-350.

51. Wang H, Zhang C, Li Y, Qi H (2006) Electrogenerated chemiluminescence detection for deoxyribonucleic acid hybridization based on gold nanoparticles carrying multiple probes. Anal Chim Acta 575: 205-211.

52. Gao F, Pan BF, Zheng WM, Ao L, Gu H (2005) Study of streptavidin coated onto PAMAM dendrimer modified magnetite nanoparticles. J Magn Magn Mater 293: 48-54.

53. Lu H, Yi G, Zhao S, Chen D, Guo L, et al. (2004) Synthesis and characterization of multi-functional nanoparticles possessing magnetic, up-conversion fluorescence and bio-affinity properties. J Mater Chem 14: 1336-1341.

54. Erdem A, Sayar F, Karadeniz H, Guven G, Ozsoz M, et al. (2007) Development of Streptavidin Carrying Magnetic Nanoparticles and Their Applications in Electrochemical Nucleic Acid Sensor Systems 19: 798-804.